Progress In Electromagnetics Research, PIER 86, 243–257, 2008

LOCALIZATION OF NARROW BAND SOURCES IN THE PRESENCE OF MUTUAL COUPLING VIA SPARSE SOLUTION FINDING

Y. Zhang

Electrical and Electronic Engineering School
Nanyang Technological University
100 Nanyang Avenue, 639798, Singapore

Q. Wan and A.-M. Huang

Department of Electronic Engineering
University of Electronic Science and Technology of China
Chengdu, Sichuan 610054, China

Abstract—Making use of the Toeplitz structure of the mutual coupling matrix of the Uniform Linear Array (ULA), estimating the direction-of-arrival (DOA) of the sources as well as the mutual coupling coefficients of the array can be formulated as a linear inverse problem, where the solution is given by the Kronecker product of the vectors with respect to the DOAs and the mutual coupling coefficients. Through mathematical manipulation, these solution vectors can be decoupled. Estimation of the DOAs is cast into the framework of sparse solution finding. To derive the solution, an alternating minimization technique is presented. The proposed method is firstly developed based on the noise free observation covariance matrix, and can be generalized to directly using the snapshots. Using the proposed method, DOA estimation is feasible even in single snapshot case. The performance of the proposed methods with covariance matrix, single snapshot and multiple snapshots are illustrated by computer simulations. Their ability to resolve closely spaced targets and the applicability to correlated sources have also been demonstrated.

1. INTRODUCTION

In practical antenna arrays, the elements affect each other through mutual coupling which significantly degrades the performance of the communication system [1–3]. Therefore, calibration techniques are developed to reduce the mutual coupling effects. Some self-calibration methods have been proposed in previous literatures. In [4], an eigen-structure based DOA estimation method for arbitrary arrays in the presence of mutual coupling, gain and phase error is proposed. However, it has been shown that this method suffers from ambiguity problem in some conditions [5]. By exploiting the special structure of the mutual coupling matrix, a self-calibration method for uniform circular array (UCA) was proposed in [6] and [7], respectively. Recently, Sellone and Serra presented a novel online mutual coupling compensation algorithm for ULA [8]. This method performs an alternating minimization procedure to compensate mutual coupling of the ULA array. However, the method is suboptimal in that it treats the mutual coupling matrix $\mathbf{M}$ and its conjugate transpose $\mathbf{M}^H$ as two independent matrices. Furthermore, this method essentially targets on calibration of the array instead of DOA estimation. Therefore, additional DOA estimation procedure is required to locate the targets.

Sparse solution finding [9–11] algorithms have shown promising performance in the field of array signal processing [12]. Our previous work have also illustrated its superiority to conventional methods in spectral estimation [13], DOA estimation in Laplacian noise environment [14] and array beamforming [15]. In this paper, we extend sparse solution finding to DOA estimation and mutual coupling calibration. It is demonstrated that estimation of the DOA and the mutual coupling coefficients can be converted to a linear inverse problem. Through some mathematical manipulation, the unknown vectors with respect to the DOA and the mutual coupling coefficients can be decoupled. By introducing an over-complete dictionary, the problem of DOA estimating is realized via sparse solution finding. The proposed method is originally developed based on the noise free covariance matrix and is generalized to directly using of the snapshots. Because the proposed methods are not eigen-structure based, it can also be used in correlated sources case.

2. PROBLEM FORMULATION

Consider that L far-field narrowband sources impinge on a M-element ULA from directions $\theta_1, \dots, \theta_L$. The complex amplitude of the lth signal, $s_l(t)$, is a complex, low-pass, wide-sense stationary random process, with zero-mean and variance σ_l^2. Take the first element as the reference. As for the signal with incident angle θ, its time delay between the mth element and the reference is $\tau_m = (m-1)d\sin(\theta)/c$, where d denotes the element spacing. Therefore, in the case of ideal array, the array signal vector, can be written as

$$\mathbf{x}(t) = \mathbf{A}\mathbf{s}(t) + \mathbf{n}(t) \tag{1}$$

where $\mathbf{A} = [\mathbf{a}(\theta_1), \ldots, \mathbf{a}(\theta_L)]$ is the so-called array manifold, and $\mathbf{a}(\theta_1) = [1, \ldots, \exp(j2\pi f \tau_L)]^T$ is the steering vector. The vector $\mathbf{n}(t)$ denotes the uncorrelated additive noise on the sensors.

Supposing that the sources are uncorrelated with each other, and independent from the noise, the covariance matrix of the array signal is given by

$$\mathbf{R}_x x = E\left[\mathbf{x}\mathbf{x}^H\right] = \mathbf{A}\mathbf{R}_{ss}\mathbf{A}^H + \sigma_n^2 \mathbf{I}_M \tag{2}$$

where $\mathbf{R}_{ss} = E[\mathbf{s}\mathbf{s}^H] = \begin{bmatrix} \sigma_1^2 & \ldots & 0 \\ 0 & \ddots & 0 \\ 0 & 0 & \sigma_L^2 \end{bmatrix}$.

To take the mutual coupling effect into account, a mutual coupling matrix $\mathbf{Q}$ is included into (1). Accordingly, the array signal vector and its covariance matrix in the presence of mutual coupling can be expressed as

$$\mathbf{y}(t) = \mathbf{Q}\mathbf{A}\mathbf{s}(t) + \mathbf{n}(t) \tag{3}$$

$$\mathbf{R}_{yy} = E\left[\mathbf{y}\mathbf{y}^H\right] = \mathbf{Q}\mathbf{A}\mathbf{R}_{ss}\mathbf{A}^H\mathbf{Q}^H + \sigma_n^2\mathbf{I}_M = \mathbf{S}_y + \sigma_n^2\mathbf{I}_M \tag{4}$$

where the noise free covariance matrix of the array signal $\mathbf{S}_y = \mathbf{Q}\mathbf{A}\mathbf{R}_{ss}\mathbf{A}^H\mathbf{Q}^H$ is defined.

For ULA discussed in this paper, the mutual coupling matrix $\mathbf{Q}$ has symmetric Toeplitz structure [8].

3. THE PROPOSED SPARSE SOLUTION FINDING ALGORITHM

Making use of the symmetric Toeplitz structure of the matrix $\mathbf{Q}$, $\mathbf{S}_y$ can be vectorized as follows:

$$\text{vec}(\mathbf{S}_y) = \overline{\mathbf{H}}\left(\text{vec}\left(\Sigma_s\right) \otimes \mathbf{c}\right) \tag{5}$$

where $\otimes$ denotes Kronecker product. $\mathbf{c} = \mathbf{q}^* \bigotimes \mathbf{q} \in \mathbf{C}^{M^2\times 1}$, $\mathbf{H}(\theta) = \mathbf{G}^*(\theta) \otimes \mathbf{G}(\theta) \in \mathbf{C}^{M^2\times M^2}$, and $\overline{\mathbf{H}} = [\mathbf{H}(\theta_1), \ldots, \mathbf{H}(\theta_L)] \in C^{M^2\times M^2 L}$ are defined. The vector $\mathbf{q} = [q_1, \ldots, q_M]^T$ completely specifies $\mathbf{Q}$. The matrix $\mathbf{G}(\theta) \in \mathbf{C}^{M\times M}$ can be computed by the sum of the following two matrices:

$$\begin{aligned}
[\mathbf{G}_1(\theta)]_{ij} &= \begin{cases} [\mathbf{a}(\theta)]_{i+j-1}, & i+j \leq M+1 \\ 0, & \text{others} \end{cases} \\
[\mathbf{G}_2(\theta)]_{ij} &= \begin{cases} [\mathbf{a}(\theta)]_{i-j+1}, & 2 \leq i \leq j \\ 0, & \text{others} \end{cases}
\end{aligned} \tag{6}$$

Using the property of Kronecker product, (5) can be reformulated as

$$\text{vec}(\mathbf{S}_y) = \overline{\mathbf{H}}_c \left(\mathbf{I}_{M^2} \otimes \sigma_{\mathbf{s}}\right) \mathbf{c} = \overline{\mathbf{H}} \left(\mathbf{I}_L \otimes \sigma_{\mathbf{s}}\right) \mathbf{c} \tag{7}$$

where

$$\begin{aligned}
\overline{\mathbf{H}}_c \;=\; &\big[\overline{\mathbf{h}}_1, \overline{\mathbf{h}}_{M^2+1}, \ldots, \overline{\mathbf{h}}_{(L-1)\times M^2+1}, \overline{\mathbf{h}}_2, \ldots, \\
&\overline{\mathbf{h}}_{(L-1)\times M^2+2}, \ldots, \overline{\mathbf{h}}_{M^2}, \ldots, \overline{\mathbf{h}}_{L\times M^2}\big],
\end{aligned}$$

$\overline{\mathbf{h}}_i$ denotes the ith column of $\overline{\mathbf{H}}$. $\mathbf{I}_{M^2}$ and $\mathbf{I}_L$ are M^2-dimensional and L-dimensional unity matrix, respectively. $\sigma_{\mathbf{s}}$ consists of the diagonal element of Σ_s.

Similarly, we may represent (3) as follows:

$$\text{vec}(\mathbf{y}(t)) = \overline{\mathbf{G}}_q \left(\mathbf{I}_M \otimes \mathbf{s}(t)\right) \mathbf{q} + \mathbf{n}(t) \tag{8}$$

where $\overline{\mathbf{G}} = [\mathbf{G}(\theta_1), \ldots, \mathbf{G}(\theta_L)]$ and

$$\begin{aligned}
\overline{\mathbf{G}}_q \;=\; &\Big[\overline{\mathbf{g}}_1, \overline{\mathbf{g}}_{M+1}, \ldots, \overline{\mathbf{g}}_{(L-1)\times M+1}, \overline{\mathbf{g}}_2, \ldots, \\
&\overline{\mathbf{g}}_{(L-1)\times M+2}, \ldots, \overline{\mathbf{g}}_M, \ldots, \overline{\mathbf{g}}_{L\times M}\Big].
\end{aligned}$$

To cast the DOA estimation problem into the framework of sparse solution finding, an over-complete representation of the matrix $\overline{\mathbf{H}}$ and $\overline{\mathbf{G}}$ in terms of all desired source DOAs are constructed, given by $\widetilde{\mathbf{H}} = \left[\mathbf{H}(\widetilde{\theta}_1), \ldots, \mathbf{H}(\widetilde{\theta}_N)\right]$, $\widetilde{\mathbf{G}} = \left[\mathbf{G}(\widetilde{\theta}_1), \ldots, \mathbf{G}(\widetilde{\theta}_N)\right]$, where N denotes the number of the angular samplings. Therefore, (7) and (8) are converted to

$$\begin{aligned}
\text{vec}(\mathbf{S}_y) &= \widetilde{\mathbf{H}}_c \left(\mathbf{I}_{M^2} \otimes \mathbf{m}\right) \mathbf{c} = \widetilde{\mathbf{H}} \left(\mathbf{I}_N \otimes \mathbf{m}\right) \mathbf{c} \\
\text{vec}(\mathbf{y}(t)) &= \widetilde{\mathbf{G}}_q \left(\mathbf{I}_M \otimes \widetilde{\mathbf{s}}(t)\right) \mathbf{q} + \mathbf{n}(t)
\end{aligned} \tag{9}$$

where $\mathbf{m}$ and $\widetilde{\mathbf{s}}(t)$ are sparse vectors, whose ith element is nonzero if and only if its corresponding $\widetilde{\theta}_i$ equals to one of the targets' DOA.

To derive the solution to (9), we firstly assume that $\mathbf{m}$ and $\widetilde{\mathbf{s}}(t)$ are fixed, and construct the cost functions as below:

$$\begin{aligned}&\min_{\mathbf{c}} \left\| \mathrm{vec}(\mathbf{S}_y) - \widetilde{\mathbf{H}}_c \left(\mathbf{I}_{M^2} \otimes \mathbf{m} \right) \mathbf{c} \right\|_2^2 \\ &\min_{\mathbf{q}} \left\| \mathrm{vec}(\mathbf{y}(t)) - \widetilde{\mathbf{G}}_q \left(\mathbf{I}_M \otimes \widetilde{\mathbf{s}}(t) \right) \mathbf{q} \right\|_2^2\end{aligned} \tag{10}$$

They have closed form solution given by

$$\begin{aligned}\mathbf{c} &= \left(\widetilde{\mathbf{H}}_c \left(\mathbf{I}_{M^2} \otimes \mathbf{m} \right) \right)^+ \mathrm{vec}(\mathbf{S}_y) \\ \mathbf{q} &= \left(\widetilde{\mathbf{G}}_q \left(\mathbf{I}_M \otimes \widetilde{\mathbf{s}}(t) \right) \right)^+ \mathrm{vec}(\mathbf{y}(t))\end{aligned} \tag{11}$$

In (11), + denotes the pseudo-inverse of the matrix.

Secondly, based on the fact that $\mathbf{m}$ and $\widetilde{\mathbf{s}}(t)$ are sparse, we use L_p norm [9] to constrain its sparsity. The cost functions are given by

$$\begin{aligned}&\min_{\mathbf{m}} \left\| \mathrm{vec}(\mathbf{S}_y) - \widetilde{\mathbf{H}} \left(\mathbf{I}_N \otimes \mathbf{c} \right) \mathbf{m} \right\|_2^2 + \lambda E^p(\mathbf{m}) \\ &\min_{\widetilde{\mathbf{s}}(t)} \left\| \mathrm{vec}(\mathbf{y}(t)) - \widetilde{\mathbf{G}} \left(\mathbf{I}_N \otimes \mathbf{q} \right) \widetilde{\mathbf{s}}(t) \right\|_2^2 + \lambda E^p(\widetilde{\mathbf{s}}(t))\end{aligned} \tag{12}$$

where $E^p(\cdot)$ represents L_p, $p \leq 1$ norm which is the diversity measurement. λ is a positive regularization parameter which controls the sparsity of the result by giving preference to solutions with small diversity measurement. Different criteria [9] can be used to determine it, including quality of fit, sparse criterion and L-curve.

The two procedures are repeated until convergence. Because the cost functions (12) are usually non-convex [9, 10], a local minimum might occur. When this happens, the sparse solution finding algorithms, such as FOCUSS [9], can be re-initialized to solve (12).

The following is the summary of the proposed algorithm.

Initial: $\mathbf{m}^{(0)}$, $k = 0$;

Computing: $\mathbf{c}^{(0)} = \left(\widetilde{\mathbf{H}}_c \left(\mathbf{I}_{M^2} \otimes \mathbf{m}^{(0)} \right) \right)^+ \mathrm{vec}(\mathbf{S}_y)$;

Updating:

$$\begin{aligned}\mathbf{W}^{k+1} &= \mathrm{diag}\left(\left| \mathbf{m}^{(k)} \right|^{1-p/2} \right), \\ \widetilde{\widetilde{\mathbf{H}}}_W^{(k+1)} &= \widetilde{\mathbf{H}} \left(\mathbf{I}_N \otimes \mathbf{c}^{(k)} \right) \mathbf{W}^{(k+1)}, \\ \mathbf{m}^{(k+1)} &= \mathbf{W}^{(k+1)} \left(\widetilde{\widetilde{\mathbf{H}}}_W^{(k+1)} \right)^T \left(\widetilde{\widetilde{\mathbf{H}}}_W^{(k+1)} \left(\widetilde{\widetilde{\mathbf{H}}}_W^{(k+1)} \right)^T + \lambda \mathbf{I}_N \right) \mathrm{vec}(\mathbf{S}_y),\end{aligned}$$

$$\mathbf{c}^{(k+1)} = \left(\widetilde{\mathbf{H}}_c\left(\mathbf{I}_{M^2}\otimes\mathbf{m}^{(k+1)}\right)\right)^{+}\mathrm{vec}(\mathbf{S}_y),$$
$$k = k+1;$$

until convergence.

The algorithm is terminated either $\|\mathbf{m}^{(k+1)}-\mathbf{m}^{(k)}\|_2^2/\|\mathbf{m}^{(k)}\|_2^2 < \epsilon$, has been satisfied, or the number of the iteration exceeds the prespecified value, where ϵ is a preset value.

To derive $\widetilde{\mathbf{s}}(t)$ in single snapshot case, we just need to make the following substitution to the updating procedure: $\mathbf{y}(t) \to \mathrm{vec}(\mathbf{S}_\mathbf{y})$, $\widetilde{\mathbf{G}} \to \widetilde{\mathbf{H}}$, $\widetilde{\mathbf{G}}_q \to \widetilde{\mathbf{H}}_c$, $\widetilde{\mathbf{s}}(t) \to \mathbf{m}$ and $\mathbf{q} \to \mathbf{c}$. If multiple snapshots are available, the iterative algorithm is easy to generalize [11] and is omitted here.

4. SOME ISSUES ON IMPLEMENTATION OF THE ALGORITHM

4.1. Computational Loads Consideration

When either the number of the array elements or the angular samplings is large, the sparse solution algorithm might be time consuming. In order to alleviate the computational burden, some alternative to the original algorithm should be implemented.

Firstly, making use of the fact that the covariance matrix $\mathbf{S}_y$ is symmetric, only the upper or lower triangle of is required to form $\mathrm{vec}(\mathbf{S}_y)$. Consequently, the number of the rows of the over-complete dictionary is reduced to $\frac{M(M+1)}{2}$. On the other hand, in order to reduce the number of the angular samplings, a coarse estimation of the DOA can be used to initialize the proposed algorithm. Also, grid refinement technique [12] can be implemented.

Secondly, for the ULA considered in this paper, a given element may be influenced by its nearby elements and the influence from the others may be neglected. Supposing only the nearest P, $P < M$ elements are taken into account, the number of the nonzero elements of $\mathbf{c}$ are only P^2. The decrease of the number of the unknown parameters favors obtaining of the correct estimation.

4.2. Acceleration of the Proposed Sparse Solution Finding Algorithm

Because the sparse solution finding algorithm is competitive, after several iterations, some elements in $\mathbf{m}^{(k)}$ which correspond to the true

DOAs may become larger than the others. Based on this observation, we propose to update $\mathbf{m}^{(k+1)}$ as follows:

$$\widetilde{\mathbf{m}}^{(k+1)} = \gamma\widetilde{\mathbf{m}}^{(k)} + (1-\gamma)\mathbf{m}^{(k+1)} \tag{13}$$

where $0 < \gamma < 1$ and

$$\widetilde{\mathbf{m}}^{(k)} = \widetilde{\mathbf{W}}^{(k+1)} \left(\widetilde{\widetilde{\mathbf{H}}}_{\widetilde{W}}^{(k+1)}\right)^T \left(\widetilde{\widetilde{\mathbf{H}}}_{\widetilde{W}}^{(k+1)} \left(\widetilde{\widetilde{\mathbf{H}}}_{\widetilde{W}}^{(k+1)}\right)^T + \lambda\mathbf{I}_N\right) \mathrm{vec}(\mathbf{S}_y).$$

$\widetilde{\mathbf{W}}^{(k+1)}$ is calculated using only the L largest values of $\mathbf{m}^{(k)}$.

The larger the γ, the faster the sparse solution can be derived. However, because large value of γ sacrifices the information of $\mathbf{m}^{(k+1)}$, the possibility of obtaining a false solution increases. Empirically, $\gamma \leq 0.3$ is preferred.

4.3. Scale Uncertainty of the Estimation

From (9), it is easy to note that for any nonzero real value a, (14) holds.

$$\begin{aligned} \mathrm{vec}(\mathbf{S}_y) &= \widetilde{\mathbf{H}}_c \left(\mathbf{I}_{M^2} \otimes \frac{1}{a}\mathbf{m}\right) a\mathbf{c} = \widetilde{\mathbf{H}} \left(\mathbf{I}_N \otimes \frac{1}{a}\mathbf{m}\right) a\mathbf{c} \\ \mathrm{vec}(\mathbf{y}(t)) &= \widetilde{\mathbf{G}}_q \left(\mathbf{I}_M \otimes \frac{1}{a}\widetilde{\mathbf{s}}(t)\right) a\mathbf{q} + \mathbf{n}(t) \end{aligned} \tag{14}$$

Thus, the derived solution using the proposed algorithm may be scaled by a constant. This constant can be estimated via $\widehat{a} = \frac{1}{M^2}\sum_{i=1}^{M^2}|c_i/c_1|$ or $\widehat{a} = \frac{1}{P^2}\sum_{i=1}^{P^2}|c_i/c_1|$ under the assumption that the true mutual coupling coefficient has been normalized with respect to the first sensor (reference).

5. COMPUTER SIMULATIONS

In this section, some computer simulations are conducted to verify the validation of the proposed methods.

In all simulations, the methods derived in Section 3 are named Covariance Based Method (CBM), Single-snapshot Based Method (SBM) and Multiple-snapshot Based Method (MBM), respectively.

We consider an ULA array with eight sensors separated by $d = \lambda/2$, where λ denotes the wavelength corresponding to the operating frequency of the narrow band sources. The sampling grid for generating the over-complete dictionary is uniform with 1° interval.

Case 1): Two closely spaced correlated narrow band sources in the far field impinge on the array from 31° and 37°, respectively. As for a given element, four nonzero mutual coupling coefficients are taken into account, i.e., $P = 4$. The mutual coupling coefficients are set to be $0.6 + 0.4j$ for the elements which are d apart, and $0.2 - 0.1j$ for the elements which are $2d$ and $3d$ apart.

Case 2): Three correlated narrow band sources with DOA 31°, 54° and 71° are assumed. Based on the necessary condition for a unique solution [8], we set $P = 3$ in this case, i.e., the mutual coefficients with the sensors which are $3d$ and more apart are neglected. The values of the coefficients are identical to those in Case 1.

5.1. Capability to Resolve Closely Spaced Sources

The signal-to-noise ration (SNR) is chosen to be 10 dB. 20 snapshots were used. With the experimental parameters given in Case 1 and Case 2, the proposed three algorithms were conducted.

The estimated spatial spectrum for case 1 is depicted in Fig. 1. It is noted that the peak of the uncalibrated MUSIC [16] spatial spectrum deviates from the true position due to the impact of the mutual coupling. Meanwhile, MUSIC is incapable to resolve the two targets.

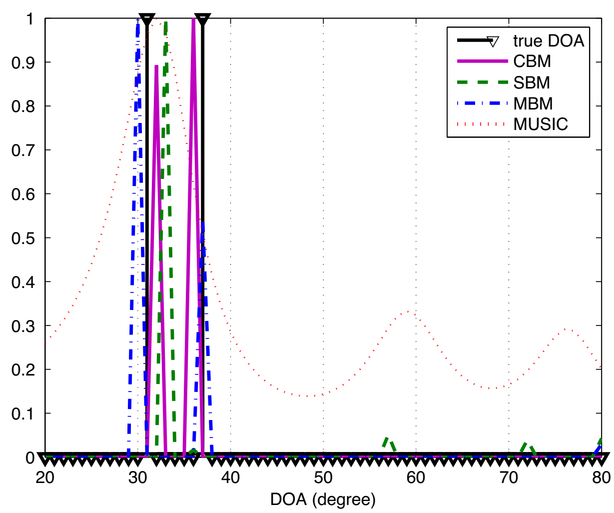

Figure 1. Estimated spatial spectrum with the proposed method compared with the uncalibrated MUSIC spectrum. Two closely spaced targets and four nonzero mutual coupling coefficients were assumed. (Case 1)

As the comparison, the proposed methods perform much better, in which CBM and MBM are capable of either locating the peaks of the spatial spectrum or resolving the two targets. As for the SBM, it can not distinguish the two closely spaces sources. However, it may provide initial guess for the other algorithms and favors their implementation. When the targets are not very close to each other, the situation becomes somewhat better for SBM. As the Fig. 2 demonstrates, all of the proposed methods can locate the three targets, in which CBM and MBM perform better.

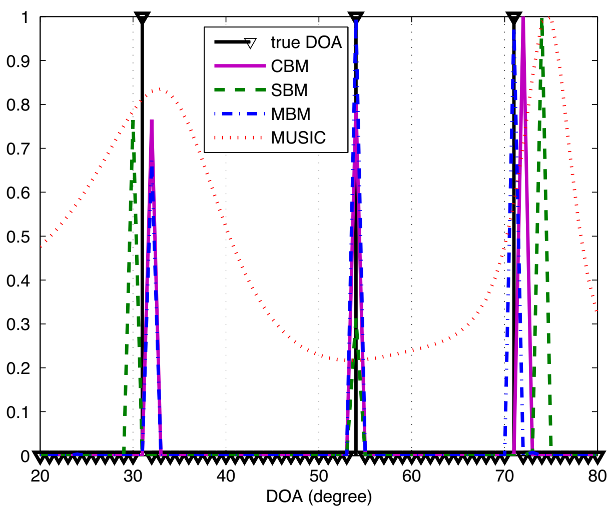

Figure 2. Estimated spatial spectrum with the proposed method compared with the uncalibrated MUSIC spectrum. Three targets and three nonzero mutual coupling coefficients were assumed. (Case 2)

5.2. Capability to Estimate c with Respect to the Coupling Coefficients

The method CBM is considered in this experiment. The capability of CBM to estimate the vector **c** is validated via computer simulations with parameters given in Case 1. The SNR is set to 10 dB.

There are $4^2 = 16$ nonzero elements in **c**. However, according to the assumed mutual coupling coefficients, some elements share identical phase. It can be counted that 9 distinct phases appear. The convergence routes of the phase of these 9 nonzero elements are shown in Fig. 3. More specifically, Fig. 4 presents the convergence route for c_2, c_3, c_{11} and c_{26}, i.e., $q_1^* q_2$, $q_1^* q_3$, $q_2^* q_3$ and $q_4^* q_2$. The algorithm was

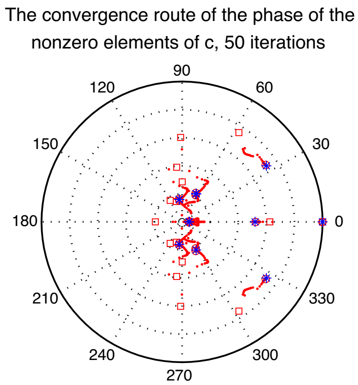

Figure 3. The convergence route of the phase of the nonzero elements of **c**. The phase is calculated as $\rho_i^{(k)} = \angle(c_i^{(k)}/c_1^{(k)}), i = 1, \ldots, 16; k = 0, \ldots, 49$. The squares and the circles denote $\rho_i^{(0)}$ and $\rho_i^{(49)}$, respectively. The asterisks denote the true phases of **c**.

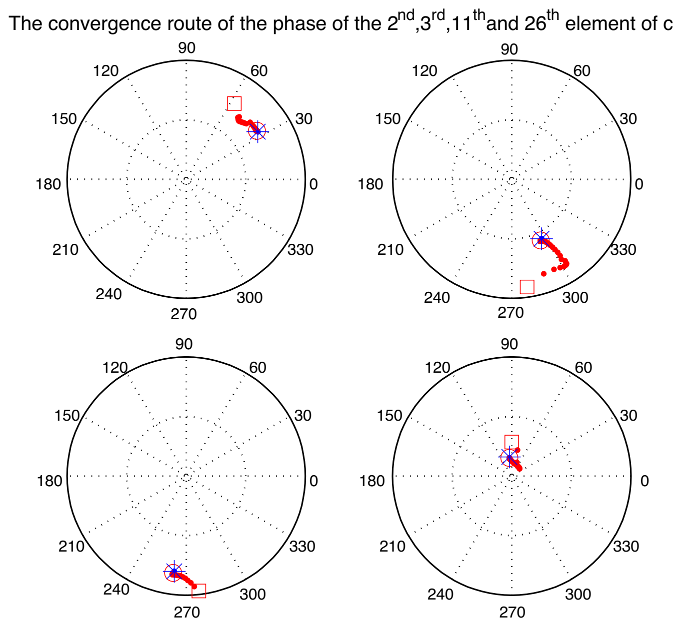

Figure 4. The convergence route of the phase of c_2, c_3, c_{11} and c_{26}.

terminated after 50 iterations. It is noted from Fig. 3 that the phase of the nonzero elements converges to the true value as the iteration goes on.

It is noted from Fig. 5 that as for the true **c**, the scaled amplitudes for all of the 16 nonzero elements are identical to 1. The closer the estimated scaled amplitudes to 1, the better the derived estimation. It is observed that when the algorithm terminates, the estimated scaled amplitudes are very close to 1. Therefore, good convergence result is achieved.

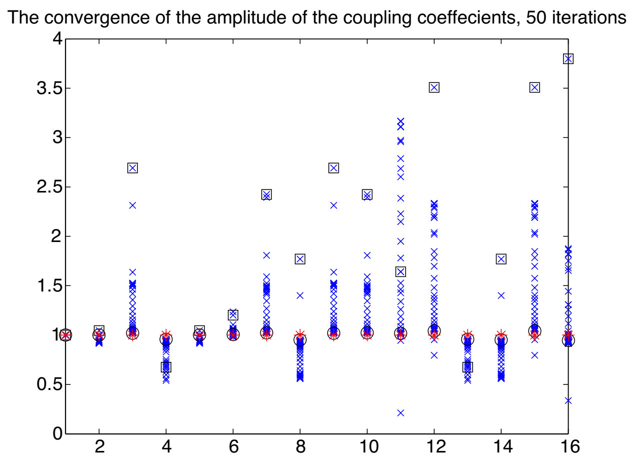

Figure 5. The convergence route of the scaled amplitude of the nonzero elements of **c**. The scaled amplitude is calculated as $\alpha_i^{(k)} = |c_i^{(k)}/c_1^{(k)}|/|c_i|, i = 1, \ldots, 16; k = 0, \ldots, 49$, where $|c_i|$ denotes the true element of **c**. The squares and the circles denote $\alpha_i^{(0)}$ and $\alpha_i^{(49)}$, respectively. The asterisks denote the true scaled amplitude of **c**.

5.3. The Correct Estimation Percentage

Since the sparse finding algorithm does not guarantee global minimum for every realization, we test its average performance in this simulation. Case 2 is used for this purpose and 100 independent trials were conducted.

Figure 6, Fig. 7 and Fig. 8 present the estimation bias using CBM, SBM and MBM with SNR equal to 10 dB, respectively. It is noted that large bias did happen, but the percentage is very low compared with the correct estimation. As discussed above, the algorithm can be re-initialized when the wrong estimation happens. To increase the accuracy of the estimation results, grid refinement technique [12] can be implemented, i.e., finer sampling grids can be used to generate the over-complete dictionary, and the searching region can be restricted to the neighbor of the coarse estimation. Accordingly, the derived estimation might be less biased.

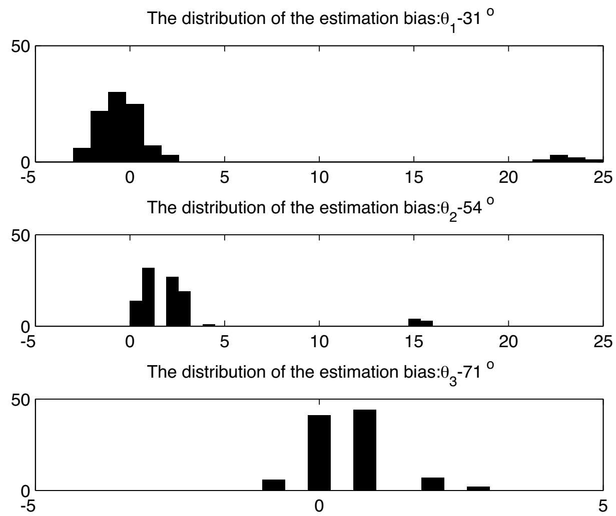

Figure 6. The distribution of the estimation bias via CBM.

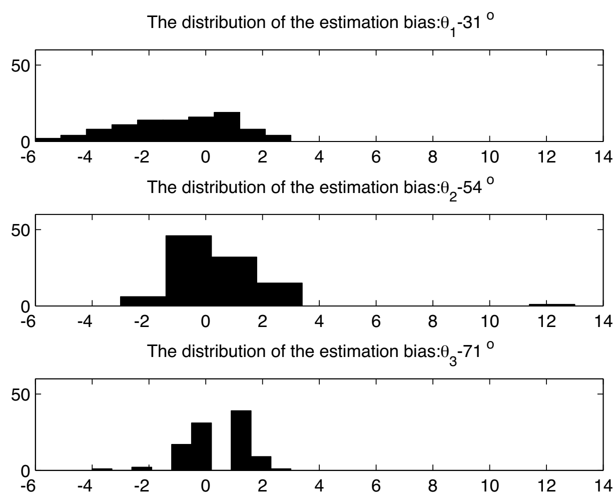

Figure 7. The distribution of the estimation bias via SBM.

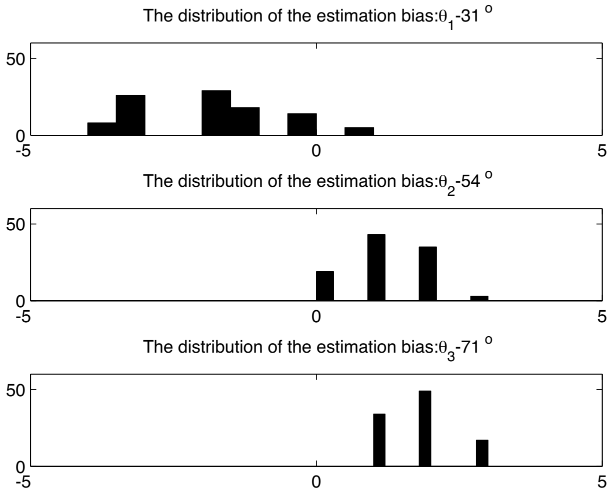

Figure 8. The distribution of the estimation bias via MBM.

6. CONCLUSIONS

In this paper, we cast the problem of localization of narrow band sources in the presence of mutual coupling into the framework of sparse solution finding. The proposed alternating minimization technique is applicable for noise free covariance matrix as well as the observation data, where single snapshot and multiple snapshots can both be used. Because the proposed methods are not eigen-structure based, they can be used for correlated sources. Computer simulations show that the proposed methods are capable of resolving closely spaced targets and do not require large number of snapshots. When the targets are not closely spaced, single snapshot is enough for the correct estimation via the proposed method. Although sparse solution finding suffers from local minimum convergence, simulations have shown that these occasions seldom occur.

ACKNOWLEDGMENT

This work was supported by a grant from the National Natural Science Foundation of China (No. 60372022, No. 60772146) and Program for New Century Excellent Talent support plan of China (No. NCET-05-0806).

REFERENCES

1. Gupta, I. J. and A. A. Ksiensiki, "Effect of mutual coupling on the performance of adaptive arrays," *IEEE Trans. on Antennas and Propagation*, Vol. 31, 785–791, Sept. 1983.
2. Abouda, A. A. and S. G. Hggman, "Effect of mutual coupling on capacity of MIMO wireless channels in high SNR scenario," *Progress In Electromagnetics Research*, PIER 65, 27–40, 2006.
3. Fallahi, R. and M. Roshandel, "Effect of mutual coupling and configuration of concentric circular array antenna on the signal-to-interference performance in CDMA systems," *Progress In Electromagnetics Research*, PIER 76, 427–447, 2007.
4. Friedlander, B. and A. J. Weiss, "Direction finding in the presence of mutual coupling," *IEEE Trans. on Antennas and Propagation*, Vol. 39, 273–284, Mar. 1991.
5. Hung, E. K. L., "A critical study of a self-calibrating direction-finding method for arrays," *IEEE Trans. on Signal Processing*, Vol. 42, 471–474, Feb. 1994.
6. Qi, C., Y. Wang, Y. Zhang, and H. Chen, "DOA estimation and self-calibration algorithm for uniform circular array," *Electronics Letters*, Vol. 41, 1092–1094, 2005.
7. Lin, M. and L. X. Yang, "Blind calibration and DOA estimation with uniform circular arrays in the presence of mutual coupling," *IEEE Antennas and Wireless Propagation Letters*, Vol. 5, 315–318, 2006.
8. Sellone, F. and A. Serra, "A novel online mutual coupling compensation algorithm for uniform and linear arrays," *IEEE Trans. on Signal Processing*, Vol. 55, 560–573, Feb. 2007.
9. Rao, B. D., K. Engan, S. F. Cotter, J. Palmer, and K. Kreutz-Delgado, "Subset selection in noise based on diversity measure minimization," *IEEE Trans. on Signal Processing*, Vol. 51, No. 3, 760–770, Mar. 2003.
10. Wipf, D. P. and B. D. Rao, "Sparse bayesian learning for basis selection," *IEEE Trans. on Signal Processing*, Vol. 52, No. 8, 2153–2164, Aug. 2004.
11. Cotter, S. F., B. D. Rao, K. Engan, and K. Kruetz-Delgado, "Sparse solutions to linear inverse problems with multiple measurement vectors," *IEEE Trans. on Signal Processing*, Vol. 53, No. 7, 2477–2488, July 2005.
12. Malioutov, D., M. Cetin, and A. S. Willsky, "A sparse signal reconstruction perspective for source localization with sensor arrays," *IEEE Trans. on Signal Processing*, Vol. 53, No. 8, 3010–

3022, Aug. 2005.

13. Zhang, Y., Q. Wan, M.-H. Wang, and W.-L. Yang, "A partially sparse solution to the problem of parameter estimation of CARD model," *Signal Processing*, Vol. 88, 2483–2491, 2008.
14. Zhang, Y., Q. Wan, H.-P. Zhao, and W.-L. Yang, "Support vector regression for basis selection in Laplacian noise environment," *IEEE Signal Processing Letters*, Vol. 14, No. 11, 871–874, Nov. 2007.
15. Zhang, Y., B. P. Ng, and Q. Wan, "Sidelobe suppression for adaptive beamforming with sparse constraint on beam pattern," *Electronics Letters*, Vol. 44, No. 10, 615–616, May 2008.
16. Schmidt, R., "Multiple emitter location and signal parameter estimation," *IEEE Trans. on Antennas and Propagation*, Vol. 34, No. 3, 276–280, May 1986.